Journal of Crystal Growth 650 (2025) 127970

Contents lists available at ScienceDirect

Journal of Crystal Growth

journal homepage: www.elsevier.com/locate/jcrysgro

Fokker-Planck equation for the crystal-size probability density in progressive nucleation and growth with application to lognormal, Gaussian and gamma distributions

M. Tomellini [a,*], M. De Angelis [a,b]

[a] Dept. of Chemical Sciences and Technologies, Tor Vergata University, Via della Ricerca Scientifica 1, 00133, Rome, Italy
[b] Superconductivity Laboratory, Dept. of Fusion and Technologies for Nuclear Safety and Security, ENEA, Via E. Fermi 45, 00044, Frascati, Rome, Italy

ARTICLE INFO

Keywords:
A1. Nucleation
A1. Growth modes
A1. Crystal Morphology
A1. Particle-size distribution function
A1. Kolmogorov-Johnson-Mehl-Avrami model

ABSTRACT

The Fokker Planck (FP) equation for the probability density function (PDF) of crystal size in phase transformations ruled by progressive nucleation and growth, has been derived. Crystals are grouped in sub-sets, we refer to as τ-crystals, where τ is the birth time of the set. It is shown that the size PDF is the superposition of the PDF of the crystal sub-sets (τ-PDFs), with weight given by the nucleation rate. The growth and diffusion coefficients entering the FP equations are estimated as a function of both τ-PDFs and nucleation rate. The functional form of these coefficients is studied for solutions of the FP equation for τ-crystals given by the lognormal, Gaussian and gamma distributions. For the first two distributions, the effect of fluctuations, nucleation rate and growth rate, on the shape of the distribution has been investigated. It is shown that for an exponential decay of the fluctuation term, the shape of the PDF is mainly governed by both the time constant for nucleation and the strength of the fluctuation. It is found that τ-PDFs given by the one-parameter gamma distributions are suitable to deal with KJMA (Kolmogorov Johnson Mehl Avrami) compliant phase transformations, where the fluctuation term is proportional to crystal size. The connection between the FP equation for the size PDF and the evolution equation for the density of crystal populations is also discussed.

1. Introduction

Crystal-size distribution function is an important quantity in the topic of crystal growth which is usually employed to characterize the morphology of the material to grow solid structures with controlled microstructures and, eventually, mechanical properties [1–3]. Modeling of this function is also significant to gain insight, through analysis of experimental data, on the underlying processes of crystal nucleation and growth [4–9]. In this ambit, among several approaches for modeling the size distribution functions, two methods are widely employed that are based on either the Fokker Planck equation (FP) (also called Kolmogorov's second equation) for the probability density function (PDF) f, or the continuity equation for the density function of crystals, N [10–14]. Specifically, by denoting with v the volume (size) of the crystal, $f(v,t)dv$ is the probability that the crystal volume is within $v, v+dv$, at time t, while $N(v,t)dv$ is the number density of crystals with volume between v and $v+dv$, at time t. The advantage of the latter method relays on the possibility to deal with the nucleation process, that is usually progressive in time, in the evolution equation for $N(v,t)$. On the other side, the FP equation allows one to study the effect of crystal-size fluctuations on the PDF [11]. The importance of fluctuations in phase transformations is evident, for example, in the case of simultaneous nucleation and growth ruled by impingement mechanism, where the final crystal-size distribution is the gamma distribution function. In the absence of fluctuations, the size distribution resembles a Dirac delta.

In ref. [12] the time evolution of the crystal-size distribution has been derived from the continuity equation with the inclusion of a source contribution to account for the nucleation process. By considering the volume of the crystal, v, and the time, t, as independent variables in the distribution function, $N(v,t)$, the equation reads:

$$\frac{\partial N(v,t)}{\partial t} = -a(t)\frac{\partial N(v,t)}{\partial v} + I(t)\delta(v-v_0). \quad (1)$$

In Eq. (1), $I(t)$ is the nucleation rate, $a(t)$ is a function of time, v_0 the size of the smallest stable nucleus and $\delta(\bullet)$ Dirac's delta. In ref. [12] it was shown that for $a(t) \propto e^{-\alpha t}$ and $I(t) \propto e^{-\beta t^2}$ the solution of Eq. (1) is close to a

* Corresponding author.
E-mail address: tomellini@uniroma2.it (M. Tomellini).

https://doi.org/10.1016/j.jcrysgro.2024.127970
Received 11 September 2024; Received in revised form 15 October 2024; Accepted 22 October 2024
Available online 24 October 2024

lognormal distribution. Integration of Eq. (1) is reported in the *Supplementary material S1* by means of the Laplace transform method and a judicious application of the shift theorem.

On one hand, in this form Eq. (1) is particularly useful since it contains explicit information on the nucleation process through the $I(t)$ function. On the other hand, it could be enlightening to get an insight into the connection between Eq. (1) and equation describing stochastic processes such as Kolmogorov's second equation usually employed for modeling the size distribution function of crystals [15–18]. Such a study is significant to establish the role of fluctuations in determining the size distribution function.

The purpose of this work is to derive a FP-like equation that allows describing the nucleation process through the explicit inclusion of the nucleation rate. Also, the approach presented here makes it possible to determine the FP equation that is consistent with Eq. (1). The method is applied to discuss the effect of fluctuations on the PDF in progressive nucleation, and examples are offered for the lognormal, Gaussian and gamma distributions

2. Results and discussion

2.1. Remarks on FP equation

We recall, in brief, that Kolmogorov's second equation gives the time evolution of the probability density function (PDF) of the stochastic variable for given value of the stochastic variable at previous time. The probability density entering Kolmogorov equation is $f(\tau,x|t,y)$, where fdy is the probability the value of the stochastic variable is between y,$y+dy$, at time t, given that its value is x at $\tau<t$. Kolmogorov's second equation reads:

$$\frac{\partial f(\tau,x|t,y)}{\partial t}=-\frac{\partial[A(y,t)f(\tau,x|t,y)]}{\partial y}+\frac{1}{2}\frac{\partial^2[B(y,t)f(\tau,x|t,y)]}{\partial y^2}, \tag{2}$$

where $f(\tau,x|t,y)\geq 0$, $\int f(\tau,x|t,y)dy=1$ and $\lim_{\Delta t\to 0}\int_{|y-x|\geq\delta} f(t-\Delta t,x|t,y)dy=0$ for any $\delta>0$. The functions $A(x,t)$ and $B(x,t)$ are linked to the first and second moments of the PDF according to:

$$A(x,t)=\lim_{\Delta t\to 0}\frac{1}{\Delta t}\int(y-x)f(t-\Delta t,x|t,y)dy \tag{3a}$$

$$B(x,t)=\lim_{\Delta t\to 0}\frac{1}{\Delta t}\int(y-x)^2 f(t-\Delta t,x|t,y)dy \tag{3b}$$

It follows that $A(x,t)$ is the mean value of the variation of the stochastic variable in time interval Δt, and $B(x,t)$ the mean value of the square of the variation of the stochastic variable. By considering in Eq. (2) ($x=0$, $\tau=0$) at the beginning of the process, an integration by parts of Eq. (2) provides the rate equation for the mean value,

$$\frac{d\langle y\rangle}{dt}=\langle A(y,t)\rangle, \tag{4}$$

where $\langle y\rangle=\int\widetilde{f}(y,t)ydy$, $\langle A(y,t)\rangle=\int\widetilde{f}(y,t)A(y,t)dy$ and $\widetilde{f}(y,t)=f(0,0|t,y)$. Therefore, the $A(y,t)$ function dictates the time dependence of the mean size. On the same token, for the mean square displacement Eq. (2) gives,

$$\frac{d\langle y^2\rangle}{dt}=2\langle yA(y,t)\rangle+\langle B(y,t)\rangle, \tag{5a}$$

that is, using Eq. (4),

$$\frac{d\langle(y-\langle y\rangle)^2\rangle}{dt}=2\langle(y-\langle y\rangle)A(y,t)\rangle+\langle B(y,t)\rangle. \tag{5b}$$

In Eqs. (4) and (5) averages are taken on the f-PDF.

2.2. FP equation for progressive nucleation

For the present analysis, in Eqs. (2)-(5) it is reasonable to choose, as stochastic variable, the crystal volume and for τ the birth time of the crystal whose initial volume is v_0. Eq. (2) is therefore suitable for describing the evolution of the PDF of the set of nuclei born within time $\tau,\tau+d\tau$ whose infinitesimal number equals $I(\tau)d\tau$. To make the notation easier, we denote this conditional PDF as $f_\tau(v,t)\equiv f(\tau,v_0|t,v)$ which is normalized according to $\int f_\tau(v,t)dv=1$ at any τ. However, because of the nucleation process, nuclei are formed continuously and the PDF of the whole population of crystals, i.e. for the entire nucleation period, is given averaging f_τ over τ [8,15,19]:

$$f(v,t)=\frac{1}{n(t)}\int_0^t I(\tau)f_\tau(v,t)d\tau, \tag{6}$$

where $n(t)=\int_0^t I(\tau)d\tau$, total number of nuclei formed up to time t, ensures normalization of the $f(v,t)$-PDF. Moreover, from Eq. (6) one receives,

$$n(t)\frac{\partial f(v,t)}{\partial t}=I(t)f_t(v,t)+\int_0^t I(\tau)\frac{\partial f_\tau}{\partial t}d\tau-I(t)f(v,t). \tag{7}$$

By noting that $f_t(v,t)=\delta(v-v_0)$, and that $\frac{\partial f_\tau}{\partial t}$ satisfies Kolmogorov's second equation (Eq. (2))[1] we eventually get,

$$\frac{\partial f(v,t)}{\partial t}=-\frac{1}{n(t)}\int_0^t I(\tau)\left[\frac{\partial[A_\tau(v,t)f_\tau(v,t)]}{\partial v}-\frac{1}{2}\frac{\partial^2[B_\tau(v,t)f_\tau(v,t)]}{\partial v^2}\right]d\tau-\frac{I(t)}{n(t)}[f(v,t)-\delta(v-v_0)]. \tag{8}$$

To make Eq. (8) comparable to Eq. (2), we define $\overline{A}(v,t)f(v,t)=\frac{\int_0^t I(\tau)[A_\tau(v,t)f_\tau(v,t)]d\tau}{n(t)}$, that is the average value of A_τ over the distribution $I(\tau)f_\tau(v,t)$:

$$\overline{A}(v,t)=\frac{\int_0^t A_\tau(v,t)[I(\tau)f_\tau(v,t)]d\tau}{\int_0^t I(\tau)f_\tau(v,t)d\tau}, \tag{9}$$

where similar definition holds for $\overline{B}(v,t)$. The fraction $\frac{I(\tau)f_\tau(v,t)d\tau}{\int I(\tau)f_\tau(v,t)d\tau}$ is the probability that a nucleation event, between $\tau,\tau+d\tau$, produces a crystal with volume in the range $v,v+dv$ at time $t>\tau$ (see also the Appendix A). Use of the $\overline{A}(v,t)$ and $\overline{B}(v,t)$ definitions in Eq. (8) leads to

$$\frac{\partial f(v,t)}{\partial t}=-\frac{\partial[\overline{A}(v,t)f(v,t)]}{\partial v}+\frac{1}{2}\frac{\partial^2[\overline{B}(v,t)f(v,t)]}{\partial v^2}-\frac{d\ln n}{dt}[f(v,t)-\delta(v-v_0)], \tag{10}$$

that is the FP equations for the f-PDF in the case of progressive nucleation. From Eq. (10) we obtain the rate equation for the average size

[1] $\frac{\partial f_\tau}{\partial t}=-\frac{\partial A_\tau f_\tau}{\partial v}+\frac{1}{2}\frac{\partial^2 B_\tau f_\tau}{\partial v^2}$.

over the f-PDF:

$$\frac{d\langle v\rangle}{dt} = \langle \overline{A}(v,t)\rangle - \frac{d\ln n}{dt}(\langle v\rangle - v_0), \tag{11}$$

with $\langle \overline{A}(v,\ t)\rangle = \int f(v,t)\overline{A}(v,t)dv = \frac{\int dv \int_0^t I(\tau)[A_\tau(v,t)f_\tau(v,t)]d\tau}{n(t)} = \frac{1}{n(t)}\int_0^t I(\tau)\frac{d\overline{v}(t,\tau)}{dt}d\tau$, where $\frac{d\overline{v}(t,\tau)}{dt} = \langle A_\tau(v,t)\rangle$ and the average is taken over the f_τ-PDF. In like manner, we get for the variance $\Psi = \langle (v-\langle v\rangle)^2\rangle$,

$$\frac{d\Psi}{dt} = 2\langle (v-\langle v\rangle)\overline{A}(v,t)\rangle + \langle \overline{B}(v,t)\rangle - \frac{d\ln n}{dt}\left[\Psi - (\langle v\rangle - v_0)^2\right]. \tag{12}$$

In the case of both $\overline{A}(t)$ and $\overline{B}(t)$ independent of volume, integration of Eqs. (11) and (12) gives

$$\langle v\rangle = v_0 + w(t) \tag{13}$$

and

$$\Psi = \frac{1}{n(t)}\left[\int_0^t \overline{B}(t')n(t')dt' + \int_0^t I(t')w(t')^2dt'\right], \tag{14a}$$

where $w(t) = \frac{1}{n(t)}\int_0^t \overline{A}(t')n(t')dt'$. Furthermore, Eq. (14a) can be reformulated in terms of $\overline{A}(t')$ and $\overline{B}(t')$ by means of the expression of $w(t)$. Recalling that $I(t) = \frac{dn}{dt}$, an integration by parts and a lengthy algebra provides, eventually,[2]

$$\Psi = \frac{1}{n(t)}\left[\int_0^t \overline{B}(t')n(t')dt' + \frac{2}{n(t)}\int_0^t \overline{A}(t')n(t')dt'\int_{t'}^t \overline{A}(t'')(n(t)-n(t''))dt''\right]. \tag{14b}$$

In the present form, the expression clearly shows how the variance of the distribution depends on both nucleation rate and fluctuation in crystal growth, $\overline{B}(t')$. In fact, the spread of the distribution is linked to the nucleation and growth process even in the absence of fluctuations during the growth ($\overline{B} = 0$). On the other side, in the model case of site-saturated nucleation (i.e. when all nuclei start growing at the same time) the contribution related to nucleation rate vanishes; in this case $\frac{dn}{dt}$ is proportional to a Dirac delta and the last term in Eq. (14b) is zero for any $t \neq 0$ (i.e. $n(t) = N_0H(t)$, with $H(\bullet)$ the Heaviside step function). As discussed below, the spread of the distribution given by Eq. (1) is not related to fluctuations but to the nucleation and growth processes.

At this point a comment is in order: with the aim of employing the FP equation to the kinetics of phase transformations by nucleation and growth, or even recrystallization [20–22], the $A_\tau(v,t)$ function has to satisfy the condition $\lim_{t\to\infty} A_\tau(v,t) = 0$. In fact, when the transformation reaches completion the mean value of the growth rate of the crystal is zero. The same behavior is expected to be shared by the τ-averaged functions, $\overline{A}(v,t)$ and $\overline{B}(v,t)$. Such a property of the A and B coefficients ensure the asymptotic limit, in time, of the PDF. The $a(t)$ function used in Eq. (1) [12] fulfills this property. Besides, when $A_\tau(v,t)$ and $B_\tau(v,t)$ are independent of τ, then $\overline{A} \equiv A(v,t)$ and $\overline{B} \equiv B(v,t)$.

Comparison between Eq. (1) and that based on the FP approach Eq. (10), is done by means of the definitions of both $N(v,t)$ and $f(v,t)$. In fact, being f a PDF and N a crystal density per crystal volume, the relationship holds,

$$f(v,t) = \frac{N(v,t)}{n(t)}. \tag{15}$$

Eq. (15) provides $\partial_t N(v,t) = n(t)\partial_t f(v,t) + f(v,t)I(t)$. Use of this equation in the continuity Eq. (1), allows one to find the differential equation for the $f(v,t)$-PDF:

$$\frac{\partial f(v,t)}{\partial t} = -\frac{\partial[a(v,t)f(v,t)]}{\partial v} - \frac{I(t)}{n(t)}[f(v,t) - \delta(v-v_0)]. \tag{16}$$

Comparison between Eqs. (16) and (10) does show that in Kolmogorov's second equation for the PDF of the set of τ-crystals, fluctuations are absent, that is $B_\tau = 0$. Furthermore, since $a(t) = \overline{A}(v,t)$ is independent of v, the $A_\tau(v,t)$ is also independent of v. For $B_\tau = 0$ and $a(t) = A_\tau(v,t)$ the evolution equation of f_τ becomes $\partial_t f_\tau(v,t) = -a(t)\partial_v f_\tau(v,t)$ that admits the solution $f_\tau(v,t) = \phi[v-\xi(t,\tau)]$, where $\phi[\bullet]$ is a function of the stated argument, $\xi(t,\tau) = \int_\tau^t a(t')dt' + c$, with c a constant, and $a(t)$ is positive definite. In other words, the shape of the distribution is conserved in time. For a nucleation event between τ and $\tau + d\tau$ the initial distribution can be described by a Dirac delta, $\phi[v-\xi(\tau,\tau)] = \delta(v-v_0)$ a relationship that implies $c = v_0$ in $\xi(t,\tau)$ and, eventually, $f_\tau(v,t) = \delta(v-\xi(t,\tau))$. Also, $\delta(v-\xi(t,\tau)) = \frac{\delta(\tau-\tau^*(v,t))}{\left|\left(\frac{\partial\xi(t,\tau)}{\partial\tau}\right)_{\tau^*}\right|} = \frac{\delta(\tau-\tau^*(v,t))}{a(\tau^*)}$ where $\tau^*(v,t)$ is the root of the equation $\xi(t,\tau^*) = v$. Therefore, the $f(v,t)$-PDF is obtained from Eq. (6) according to

$$f(v,t) = \frac{1}{\left[\int_0^t I(t')dt'\right]}\frac{I[\tau^*(v,t)]}{a[\tau^*(v,t)]}. \tag{17}$$

For $a(t) = \gamma e^{-\alpha t}$ we get $\tau^*(v,t) = -\frac{1}{\alpha}\ln\left[\frac{\alpha}{\gamma}(v-v_0) + e^{-\alpha t}\right]$ with the constraint $v < \xi(t,0) = v_0 + \frac{\gamma}{\alpha}(1-e^{-\alpha t})$ being τ^* positive definite.[3]

In the following, the nucleation rate is of the functional form, $I(t) = I_0e^{-\beta t^n}$. This choice is justified by the fact that the stretched exponential is appropriate for modeling phase transformations ruled by nucleation and growth [12,22,23]. For a stretched exponential nucleation rate, Eq. (17) becomes

$$f(v,t) = \frac{1}{n(t)}\frac{e^{(-1)^{n+1}\beta\left(\frac{1}{\alpha}\ln\left[\frac{\alpha}{\gamma}(v-v_0)+e^{-\alpha t}\right]\right)^n}}{\alpha(v-v_0)+\gamma e^{-\alpha t}}\chi(v)_{v_0,\xi(t,0)}, \tag{18}$$

with $\chi_{a,b}(x)$ characteristic function ($\chi_{a,b}(x) = 1, a < x < b$ and $\chi_{a,b}(x) = 0$ elsewere). For $n = 2$ the asymptotic behavior of Eq. (18) resembles the lognormal distribution. Eq. (18) is consistent with the $N(v,t)$ distribution derived in ref. [12] (see also the *Supplementary Material S1*). As stressed in ref. [12] at $n = 2$ the main difference of this distribution with the lognormal is given by the argument of the exponential and by the cut-off in the v domain due to the characteristic function.

2.3. Numerical computations

This section is devoted to an application of the results of sect.2.2 to a variety of cases in dependence of the functional form of A and B coefficients. The numerical computations presented here, have been performed using the *Wolfram Mathematica* package.

2.3.1. A and B coefficients depending only on time

The approach above discussed allows one to study the effect of fluctuations, on the PDF, during the growth. To account for the spread of the distribution, the higher order derivative term has to be considered, implying $B_\tau(v,t) \neq 0$ in Eqs. (2), (8). Equation 10 shows that fluctuations can be considered, in the differential equation for the $N(v,t)$ distribution Eq. (1), through the extra term $\frac{1}{2}\frac{\partial^2[\overline{B}(v,t)N(v,t)]}{\partial v^2}$. However, to find the f-PDF it is more profitable, in this case, to solve the differential equation for f_τ and use Eq. (6). For A_τ and B_τ independent of volume the solution of Kolmogorov's second equation provides (see also the Appendix B)

[2] In this derivation use is done of the relationships: $\int_0^t f(t')dt'\int_0^{t'} g(t'')dt'' = \int_0^t g(t'')dt''\int_{t''}^t f(t')dt'$ and $\left(\int_0^t f(t')dt'\right)^2 = 2\int_0^t f(t')dt'\int_{t'}^t f(t'')dt''$.

[3] The time τ^* is solution of the equation $\xi(t,\tau^*) = v$, where $\xi(t,\tau) = v_0 + \gamma\int_\tau^t e^{-\alpha x}dx = v_0 + \frac{\gamma}{\alpha}(e^{-\alpha\tau} - e^{-\alpha t})$.

$$f_\tau(v,t) = C(t,\tau)e^{-\frac{(v-\xi(t,\tau))^2}{4\varphi_2}}, \tag{19}$$

where $\xi(t,\tau) = v_0 + \varphi_1(t,\tau)$, $\varphi_1(t,\tau) = \int_\tau^t a_\tau(x)dx$, $C(t,\tau) = \frac{1}{\sqrt{4\pi\varphi_2}}$ and $\varphi_2(t,\tau) = \int_\tau^t b_\tau(x)dx$ with $b_\tau(t) = B_\tau(t)/2$. Since $v \geq 0$, Eq. (19) is the solution for the normalized PDF provided $f_\tau(0,t) \cong 0$. Furthermore, from Eq. (6) it follows that $\langle v\rangle = \frac{1}{n}\int_0^t I(\tau)\bar{v}(t,\tau)d\tau$ and $\langle v^2\rangle = \frac{1}{n}\int_0^t I(\tau)\overline{v^2}(t,\tau)d\tau$, that leads, after use of Eq. (19), to

$$\langle v\rangle = \frac{1}{n(t)}\int_0^t I(\tau)\xi(t,\tau)d\tau \tag{20}$$

$$\begin{aligned}\Psi &= \langle v^2\rangle - \langle v\rangle^2 \\ &= \frac{2}{n(t)}\int_0^t I(\tau)\varphi_2(t,\tau)d\tau + \frac{1}{n^2(t)}\left[n(t)\int_0^t I(\tau)\xi^2(t,\tau)d\tau \right. \\ &\quad \left. - \left(\int_0^t I(\tau)\xi(t,\tau)d\tau\right)^2\right].\end{aligned} \tag{21}$$

Inserting the $\xi(t,\tau)$ expression in Eq. (21) and the relation $I(t) = dn/dt$ in an integration by parts, it is possible to show that Eqs. (20) and (21) coincide with Eqs. (14a)–(14b) derived above (see also the *Supplementary Material S2*).

In the case $f_\tau(0,t) \neq 0$ ($t > 0$) an approximate PDF is given by Eq. (19) with $C(t,\tau) = (\pi\varphi_2(t,\tau))^{-1/2}\left[1 + \mathrm{erf}\left(\frac{\varphi_1(t,\tau)}{2\varphi_2(t,\tau)^{1/2}}\right)\right]^{-1}$ as normalization term. An estimate of the error due to this assumption is given by $\Delta = \left(\frac{1}{2} - \frac{1}{1+\mathrm{erf}\left(\frac{\varphi_1(t,\tau)}{2\varphi_2(t,\tau)^{1/2}}\right)}\right)$. Computation of this factor provides uncertainties of a few percent, as displayed in Fig. 1 where the function is studied in terms of reduced variables (see below).

Application of Eqs. (6),(19) allows to include fluctuation term in Eq. (1). By considering $a_\tau(t) = a(t) = \gamma e^{-\alpha t}$ and $b_\tau(t) = b(t)$, the PDF is computed according to

$$f(v,t) = \frac{1}{n(t)}\int_0^t \frac{I(\tau)}{\sqrt{\pi\varphi_2(t,\tau)}\left[1 + \mathrm{erf}\left[\frac{\varphi_1(t,\tau)}{2\varphi_2(t,\tau)^{1/2}}\right]\right]} e^{-\frac{(\xi(t,\tau)-v)^2}{4\varphi_2(t,\tau)}} d\tau. \tag{22}$$

For the stretched exponential, $I_0 e^{-\beta t^2}$, Eq. (22) is the superposition (at $t < \infty$) of lognormal-like and normal distributions. In this case $N(v,t)$ deviates from the lognormal distribution to an extent that depends upon b. In fact, the Dirac delta distribution, $\delta(\xi - v)$, is obtained in the limit $\varphi_2 \to 0$ (i.e. $B \to 0$) and Eq. (22) reduces to Eq. (18) (see also the Appendix B). In the following, we study the behavior of the distribution for the nucleation rate $I(t) = I_0 e^{-\beta t^2}$ and $b(t) = b_0 e^{-t/\tau_F}$, with constant b_0 and τ_F, that is $\varphi_2(t,\tau) = b_0\tau_F\left(e^{-\tau/\tau_F} - e^{-t/\tau_F}\right)$. Through the relationship $\tau(\xi) = -\frac{1}{\alpha}\ln\left[(\xi - v_0)\frac{\alpha}{\gamma} + e^{-\alpha t}\right]$ we change, in Eq. (22), the integration variable from τ to $x = \xi/\gamma\tau_G$ and define the characteristic times $\tau_G = \alpha^{-1}$ and $\tau_N = \beta^{-1/2}$, the reduced variables, $t' = t/\tau_G$, $v' = v/\gamma\tau_G$ and the dimensionless quantities $\tau'_N = \tau_N/\tau_G$, $\tau'_F = \tau_F/\tau_G$ and $\eta = \frac{\gamma\tau_G}{\sqrt{\tau_F b_0}}$. Eq. (22) becomes, eventually

$$f(v',t') = \frac{2\eta}{\pi\tau'_N \mathrm{erf}\left(\frac{t'}{\tau'_N}\right)}\int_0^{1-e^{-t'}} \frac{e^{-\left[\frac{1}{\tau'_N}\ln(x+e^{-t'})\right]^2} e^{-\eta^2\frac{(x-v')^2}{4q(x,t')}}}{\sqrt{q(x,t')}(x+e^{-t'})\left[1 + \mathrm{erf}\left(\frac{\eta x}{2\sqrt{q(x,t')}}\right)\right]} dx, \tag{23a}$$

where $q(x,t') = (x + e^{-t'})^{\frac{1}{\tau'_F}} - e^{-\frac{t'}{\tau'_F}}$, and $v_0 = 0$ was considered. The asymptotic distribution is the superposition of Gaussian functions according to

$$f(v') = \frac{2\eta}{\pi\tau'_N}\int_0^1 \frac{e^{-\left[\frac{1}{\tau'_N}\ln(x)\right]^2} e^{-\eta^2\frac{(x-v')^2}{4x^{1/\tau'_F}}}}{x^{1+\frac{1}{2\tau'_F}}\left[1 + \mathrm{erf}\left(\frac{\eta x^{1-\frac{1}{2\tau'_F}}}{2}\right)\right]} dx. \tag{23b}$$

Typical behavior of the asymptotic limit of Eq. (23a) is shown in Fig. 2 for several values of the parameters. The time constant for fluctuation was chosen of the order of magnitude of that for particle growth although, as discussed below, τ'_F does not affect the distribution significantly. It stems that the shape of the asymptotic PDF changes from a Gaussian to a truncated lognormal distribution depending on parameter values. The truncated lognormal function is recovered at large η and τ'_F, being η the more critical quantity in this context (Fig. 2a-b). In fact, when fluctuations are absent Eq. (1) holds true and the PDF admits a cut-off in the v domain, as also pointed out in ref. [12]. Under this circumstance, the asymptotic solution of the FP equation is the truncated lognormal, namely Eq. (18) in the limit $t \to \infty$. In fact, for $b_0 \to 0$ and $\eta \gg 1$ Eq. (23b) reduces to the asymptotic limit of Eq. (18). Moreover, a change in the time constant for nucleation affects the position of the maximum of the distribution that shifts to lower v' values with increasing τ'_N (Fig. 2c-e). Fig. 3 displays the asymptotic behaviors of the PDFs which are in fair agreement with either a Gaussian or a lognormal

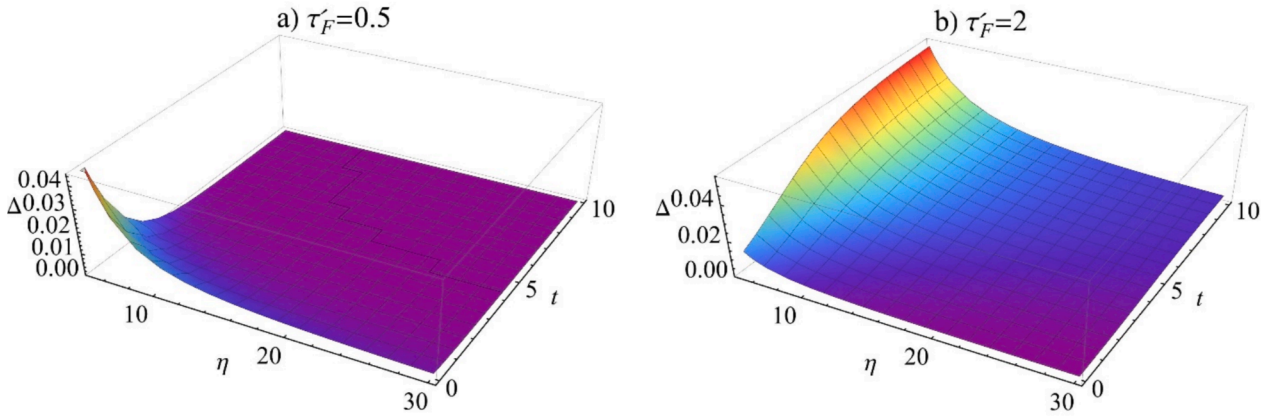

Fig. 1. 3D plot of the uncertainty, $\Delta(\eta,t)$, introduced to ensure normalization of the τ-PDF in Eq. (19). In the plot t is the reduced time, η gives a measure of the strength of the fluctuation term and τ'_F defines the time dependence of fluctuations.

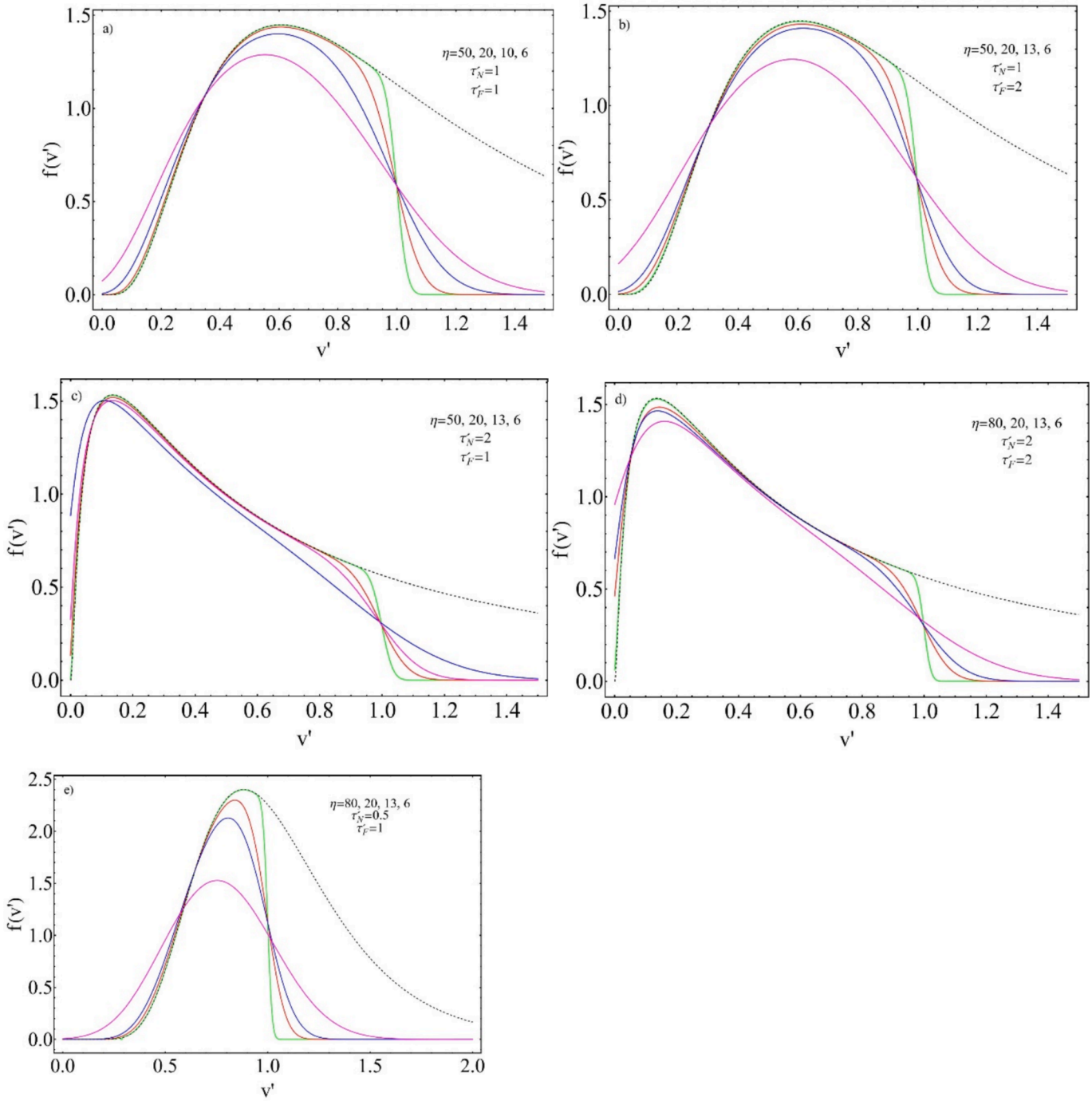

Fig. 2. Behavior of the asymptotic PDF for progressive nucleation with A and B coefficients depending on time, only. The nucleation rate is in the form of a stretched exponential with $n = 2$, as proposed in [12], to get a lognormal-like function. In all graphs, black dashed curve is the lognormal distribution. The PDFs were computed varying η, τ'_F and τ'_N. In each graph, the decreasing of η is represented by the following sequence: green, red, blue and magenta. At large η, green curves, the PDFs approach the "deterministic" solution (Eq. (18)) that is a truncated lognormal. The time constant for nucleation (τ'_N) affects the shape of the distribution to a greater extent compared to that of fluctuation (τ'_F).

distribution. The transition to one of the two distributions is mainly ruled by η. In the plot, the solid symbols are the PDF computed from Eq. (23b) and dashed (solid) line the best fit to the points of lognormal (Gaussian) distribution.

Asymptotic PDFs for a simple exponential decay of the nucleation rate are displayed in Fig. 4, for the same $A(t)$ and $B(t)$ coefficients of Fig. 2. Even in this case, the nucleation time constant τ'_N strongly affects the shape of the distribution. For $\tau'_N < 1$ the PDF becomes more symmetric the lower τ'_N and η, to become nearly uniform as $\tau'_N \to 1$. On the other hand, for $\tau'_N > 1$ the distribution is a decreasing function of v and does not exhibit any maximum.

2.3.2. *A and B coefficients depending on size and time*

2.3.2.1. Lognormal f_τ-PDF. The approach discussed in sect.2.3.1, based on either the f_τ-PDF or the continuity equation (Eq. (1)), does show how the lognormal-like PDF stems from an appropriate choice of nucleation and growth rates (a and A), in the absence of fluctuations. Specifically, I

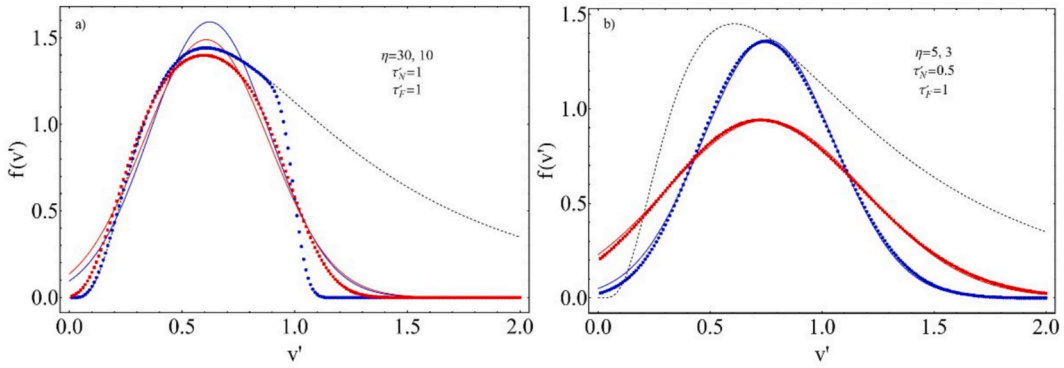

Fig. 3. Best fit of either lognormal (black dashed lines) or Gaussian (blue and red solid lines) distributions to asymptotic PDF computed through Eq. (23b) (blue and red solid symbols). The transition to one of the two distributions is mainly ruled by η. In each graph, the decreasing value of η is represented by the following sequence: blue and red.

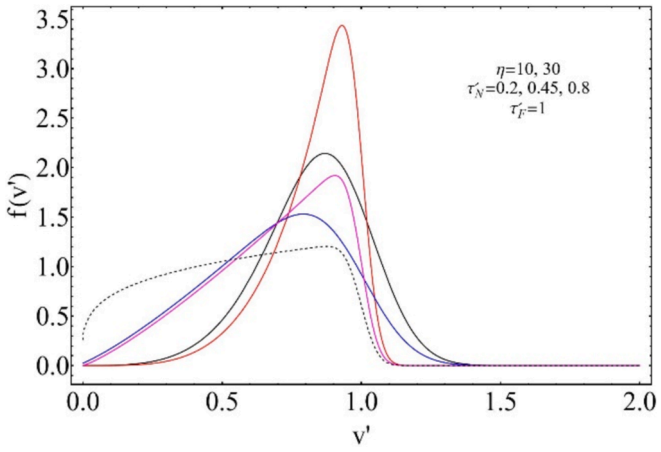

Fig. 4. Behavior of the asymptotic PDF for progressive nucleation with A and B coefficients independent of crystal size. The nucleation rate is a simple exponential decay with reduced time constant τ'_N: $I(t') = I_0 e^{-t'/\tau'_N}$. Parameter values are: $\eta = 10$, $\tau'_N = 0.2$ (black solid line), $\tau'_N = 0.45$ (blue solid line); $\eta = 30$, $\tau'_N = 0.2$ (red solid line), $\tau'_N = 0.45$ (magenta solid line), $\tau'_N = 0.8$ (black dashed line).

and A were only functions of running time, t, according to a stretched exponential with exponent 2 and 1, respectively. Also, in this case the f_τ-PDF was a Dirac delta. An interesting approach proposed in ref. [17] allows one to derive the lognormal distribution, directly from the FP equation for the f_τ-PDF, by choosing $A_\tau(t,v) = a_1(t)v$ and $B_\tau(t,v) = 2b_1(t)v^2$, where $a_1(t)$ and $b_1(t)$ are positive definite functions. The integration of the equation, that is based on a change of variables (see the *Supplementary Material S3* for details), leads to the lognormal distribution,

$$f_\tau(v,t) = \frac{1}{v\sqrt{4\pi\varphi(t,\tau)}} e^{-\frac{\rho^2}{4\varphi(t,\tau)}}, \tag{24}$$

where $\rho = \ln v + \varphi(t,\tau) - \int_\tau^t a_1(t')dt'$ and $\varphi(t,\tau) = \int_\tau^t b_1(t')dt'$. In the limit $t \to \tau$, i.e. $\varphi \to 0$, Eq. (24) gives the initial Dirac delta distribution. According to the general meaning of $a(v,t)$ and $b(v,t)$ (Eqs. (4), (5a)), we obtain $\frac{d\langle v\rangle}{dt} = \langle v\rangle a_1(t)$ and $\frac{d\langle v^2\rangle}{dt} = 2\langle v^2\rangle(a_1(t) + b_1(t))$ that lead to the following moments of the τ-PDF:

$$\langle v\rangle = e^{\int_\tau^t a_1(t')dt'} \tag{25a}$$

$$\langle v^2\rangle = e^{2\int_\tau^t [a_1(t') + b_1(t')]dt'}. \tag{25b}$$

In the limit $B_\tau \to 0$ (i.e. $b_1 \to 0$) Eq. (24) reduces to $f_\tau(v,t) = v^{-1}\delta(\ln v - \ln\bar{v}(t,\tau))$ where Eq. (25a) was used. This is the solution of FP equation without fluctuation term (see also the Appendix C). To be suitable for modeling phase transformations that reach completion, the convergence of the integrals $\int_0^\infty a_1(t')dt'$ and $\int_0^\infty b_1(t')dt'$ is required, this being a constraint on the functional form of $a_1(t)$ and $b_1(t)$. The exponential functions $a_1(t) = \omega e^{-t/\tau_G}$ and $b_1(t') = \sigma e^{-t/\tau_F}$, like those in the previous section, are both physically acceptable.

Eqs. (6), (24) give the following PDF:

$$f(v,t') = \frac{K'}{\tilde{n}(t')}\frac{1}{v}\int_0^{1-e^{-t'}} \frac{I[-\tau_G \ln(x+e^{-t'})]}{\sqrt{q(x,t')}(x+e^{-t'})} e^{-\left[\frac{1}{\omega\tau_G}\ln v + \frac{\omega\tau_G}{\eta^2}q(x,t') - x\right]^2 \eta^2/4q(x,t')} dx \tag{26}$$

where $x = \left(e^{-\tau/\tau_G} - e^{-t/\tau_G}\right)$, $\eta = \frac{\omega\tau_G}{\sqrt{\sigma\tau_F}}$ and $K' = \frac{\eta}{\omega\sqrt{4\pi}}$. For nucleation rate given by an exponential decay, $I(\tau) = I_0 e^{-\tau/\tau_N} = I_0 e^{\frac{1}{\tau'_N}\ln(x+e^{-t'})}$, we obtain

$$f(v,t') = \frac{\eta}{\sqrt{4\pi}\omega\tau_G\tau'_N(1-e^{-t'/\tau'_N})}\frac{1}{v}\int_0^{1-e^{-t'}} \frac{e^{-\left[\frac{1}{\omega\tau_G}\ln v + \frac{\omega\tau_G}{\eta^2}q(x,t') - x\right]^2 \eta^2/4q(x,t')}}{\sqrt{q(x,t')}(x+e^{-t'})^{1-\frac{1}{\tau'_N}}} dx, \tag{27}$$

with asymptotic limit

$$f(v) = \frac{\eta}{\sqrt{4\pi}\omega\tau_G\tau'_N}\frac{1}{v}\int_0^1 \frac{e^{-\left[\frac{1}{\omega\tau_G}\ln v + \frac{\omega\tau_G}{\eta^2}x^{1/\tau'_F} - x\right]^2 \eta^2/4x^{1/\tau'_F}}}{\left(x^{1+\frac{1}{2\tau'_F}-\frac{1}{\tau'_N}}\right)} dx. \tag{28}$$

According to Eq. (25a), the term $\omega\tau_G$ in Eqs.(26), (27), (28) is linked to the asymptotic value of mean crystal size at $\tau = 0$: $\bar{v}(0,\infty) = e^{\omega\tau_G}$. In Fig. 5 we report computations of the $f(v)$-PDF by means of Eqs. (28) for several values of the parameters, η, $\omega\tau_G$ and reduced time constants for nucleation and fluctuation, τ'_F and τ'_N. Differently to the case discussed in the previous section, in the present one the deviation of the distribution from lognormal is due to the nucleation process. In fact, Fig. 5a does show that for $\tau'_N \ll 1$ the distribution is nearly lognormal and that τ'_N is the main parameter determining this behavior of the PDF.

The effect of τ'_F is to shift the maximum of the PDF to larger values the lower the time constant (Fig. 5b). In addition, for the considered a_1 function, the higher the intensity of fluctuation, i.e. $\sigma\tau_F$, the lower η, which implies a greater variance of the distribution. This is shown in Fig. 6, where the standard deviation, $(\langle v^2\rangle - \langle v\rangle^2)^{1/2}$, has been plotted as

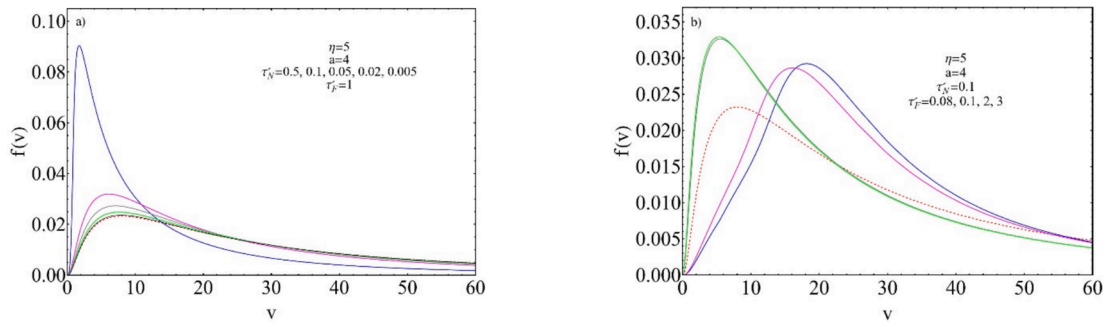

Fig. 5. Asymptotic PDF computed using Eq. (28) at $\eta = 5$, $a = \omega\tau_G = 4$. In a) the curves refer to several decreasing values of τ'_N (in order: blue, magenta, gray, green and black solid lines) and $\tau'_F = 1$, while in b) to several increasing values of τ'_F (in order: blue, magenta, gray and green solid lines) and $\tau'_N = 0.1$. In both panels the red-dashed line is the symptotic lognormal for $\eta = 5$ and $a = 4$. In the computation the nucleation rate matches an exponential decay.

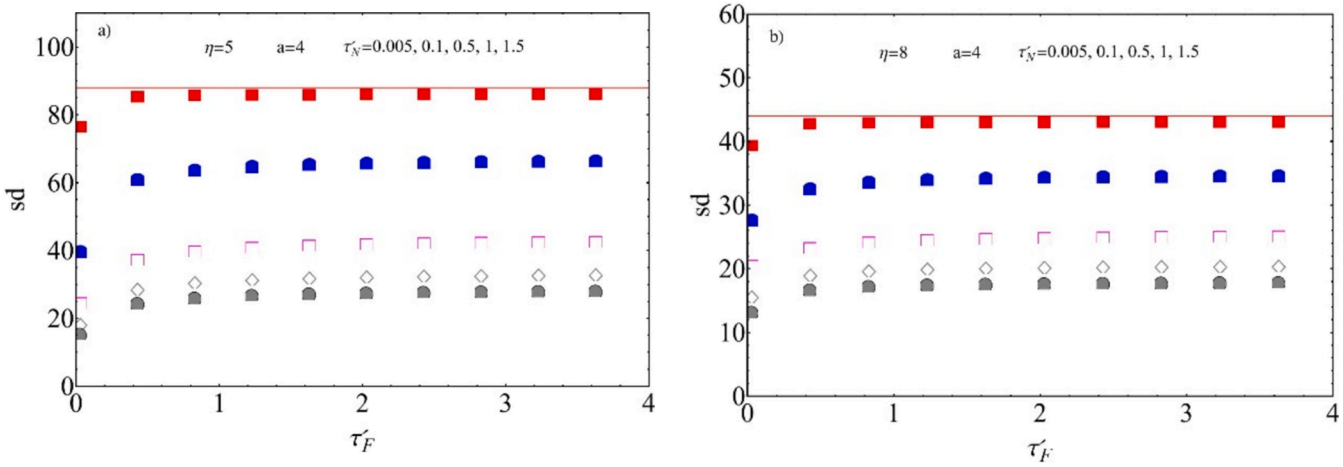

Fig. 6. Standard deviation of the asymptotic distribution Eq. (28), as a function of the reduced time constant for fluctuation, τ'_F. Computations were done for the same values of τ'_N and $a = \omega\tau_G = 4$ and $\eta = 5$ (panel a) and $\eta = 8$ (panel b): red solid squares ($\tau'_N = 0.005$), blue solid squares ($\tau'_N = 0.1$), magenta empty squares ($\tau'_N = 0.5$), gray empty diamonds ($\tau'_N = 1$) and dark gray solid circles ($\tau'_N = 1.5$). In the figures, the red straight line marks the standard deviation of the lognormal-type PDF for $\tau = 0$.

a function of τ'_F by varying τ'_N and η. The trend of the standard deviation with τ'_F indicates that: i) the approach of the PDF to the lognormal is mainly ruled by τ'_N and ii) the standard deviation decreases with increasing η and τ'_N, and with decreasing τ'_F. In the figure, the red line is the value of the standard deviation of the PDF of τ- crystals for $\tau = 0$ (Eq. (24)).

2.3.2.2. Gamma f_τ-PDF and the classical KJMA approach. This subsection is devoted to the FP equation suitable for describing crystal-size PDF in KJMA compliant transformations. In this approach, nuclei form at random throughout the volume, their position is fixed in space. Once formed, nuclei start growing, isotropically, and give rise to crystals. The growth is ruled by impingement, namely when two growing crystals collide, their growth stops at the common interface. The KJMA model, based on the Poisson process in space, is solved analytically. It allows one to compute [22,23]: i) the time evolution of the amount of the transformed phase, ii) the kinetics of growth of the mean volume of the crystals and iii) the time evolution of the nucleation rate of actual nuclei, that is the stretched exponential employed in previous sections. It is worth reminding that in KJMA model two nucleation rates are considered, namely that of actual nuclei and that comprehensive of phantom nuclei [15,24–26]. In the classical KJMA model, the former is a stretched exponential and the latter a constant.

In the KJMA compliant growth fluctuations are present because the spatial arrangement of nuclei is random. Since the rate of crystal growth is constant and upon collision their growth stops at the common interface, it follows that the volume of a single crystal depends on the local arrangement of neighboring crystals, that is stochastic in nature. In fact, the crystal-size PDF exhibits a dispersion in crystal size even for site-saturated nucleation. Computer simulations do show that in this case the asymptotic PDF (i.e. when transformation is completed) is the one-parameter gamma PDF [8,9,27], that is appropriate for describing the Poisson-Voronoi tessellation of space. Consequently, in progressive nucleation crystals belonging to the same τ-population are different in size, with f_τ-PDF's that deviate from Dirac delta. Therefore, a fluctuation term must be considered in the FP equation for the f_τ in KJMA growth.

In the case of KJMA transformations with progressive nucleation, the kinetics of the mean volume of τ-crystals, $\bar{v}(t,\tau)$ (see Section 2.2), gives information on the functional form of $A_\tau(v,t)$. This issue has been studied in ref. [15] where it has been shown that, for constant nucleation (phantom included) and growth rates in 3D, $\bar{v}(t,\tau) = \bar{v}(\infty,\tau)\left[1 - e^{-b(\tau)(t-\tau)^\kappa}\right]$ with κ a constant and $b(\tau)$ a slow varying function of τ. In terms of the dynamical variable $\xi = b(\tau)(t-\tau)^\kappa$, the A coefficient is therefore given through Eq. (4) according to $A_\tau(v,\xi) = \bar{v}(\infty,\tau) - v$. In ref. [15] it has been demonstrated, using the method based on the orthogonal-polynomial expansion of the PDF, that the solution of the FP equation of τ-crystals, for the $A_\tau(v,\xi)$ above and $B_\tau(v,\xi) \cong cv$ (with c nearly constant), is the one-parameter gamma distribution:

$$f_\tau(v,t) = \frac{{\alpha_\tau}^{\alpha_\tau}}{\Gamma(\alpha_\tau)} \frac{v^{\alpha_\tau - 1}}{\bar{v}(t,\tau)^{\alpha_\tau}} e^{-\alpha_\tau \frac{v}{\bar{v}(t,\tau)}}, \tag{29a}$$

where $\Gamma(\bullet)$ is the gamma function and $\alpha_\tau = 2\overline{v}(\infty,\tau)/c$. In Eq. (29a) reduced time and volume are used. In the classical KJMA theory for 3D-transformations the actual nucleation rate is $I(\tau) = I_0 e^{-\tau^4}$, that implies measuring time in τ_N units (see previous sections and [15]). The $\overline{v}(\infty,\tau)$ expression was computed in ref. [15] according to:

$$\overline{v}(\infty,\tau) = \frac{1}{4}e^{-\tau^4}\left(\tau^2\Gamma\left(\frac{1}{4},\tau^4\right) - 2\tau\Gamma\left(\frac{2}{4},\tau^4\right) + \Gamma\left(\frac{3}{4},\tau^4\right)\right), \tag{29b}$$

where $\Gamma(a,b) = \int_b^\infty x^{a-1}e^{-x}dx$ is the incomplete gamma function. The behavior of both $\overline{v}(\infty,\tau)$ and α_τ is displayed in Fig. 7 and shows that the two functions are nearly proportional.

The PDF for KJMA compliant transformation, $f(v,t)$, is computed using Eqs. (6), (29a), with the actual nucleation rate above reported. Fig. 8 shows the computed PDFs for several values of the reduced time. Notably, these distributions are in very good agreement with the outputs of computer simulations of KJMA transformations [15] (and references therein). The degree of transformation (volume of transformed phase divided by total volume) is 6 % for $t = 0.5$, 34 % at $t = 0.8$ and 98 % at $t = 1.4$ (close to the asymptotic value). In the same panel the dashed line is the asymptotic PDF for KJMA transformation with site-saturated nucleation. Worthy to note is the completely different behavior of the functions. For site saturated nucleation the PDF, in 1-3D, is in excellent accord with the Gamma distributions [8,28].

Because of the τ-dependence of $\overline{v}(\infty,\tau)$, for the KJMA model the average value $\overline{A}(v,t)$ differs from the A_τ coefficient of the FP equation for f_τ. The $\overline{A}(v,t)$ function is reported in Fig. 9 for various values of time. In the limit $t\to 0$ the function approaches the linear behavior of $A_0 = \overline{v}(\infty,0) - v$, and exhibits a maximum as time increases.

It is worth noticing that the A and B coefficients employed in sect.2.2.1 and 2.3.2.1 are not suitable for modeling the PDF of a classical KJMA transformation (i.e. with constant rates of both nucleation and growth). This outcome is quite evident based on the asymptotic behavior of the PDF for simultaneous nucleation (PDF of τ-crystals). In fact, when transformation is completed, crystals give rise to a subdivision of space that is the Poisson-Voronoi tessellation with a gamma distribution PDF.

3. Final remarks and Conclusions

In the previous section we have shown how the PDF is ruled by the interplay between nucleation rate and $\tau-$ PDF, the latter being related to crystal growth. For this reason, use of the present approach for modeling experimental PDFs requires the knowledge of, at least, one of these two quantities. For instance, from the knowledge of $I(t)$, the PDF

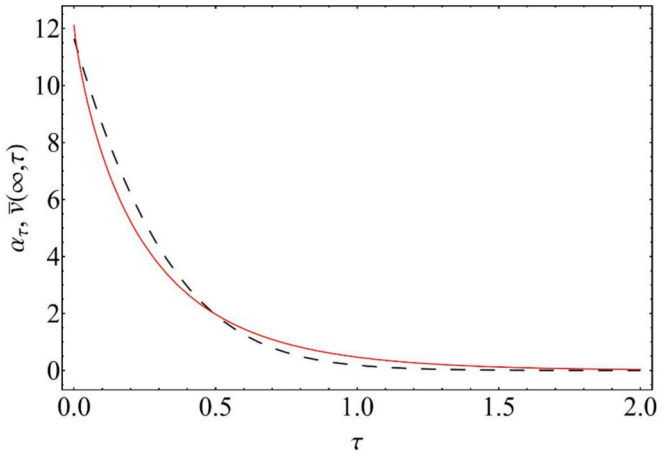

Fig. 7. Plot of the α_τ (red solid line) and $\overline{v}(\infty,\tau)$ (black dashed line) quantities as a function of reduced time τ. The asymptotic value of the τ-crystal population has been multiplied by a constant factor ($2/c \cong 30$).

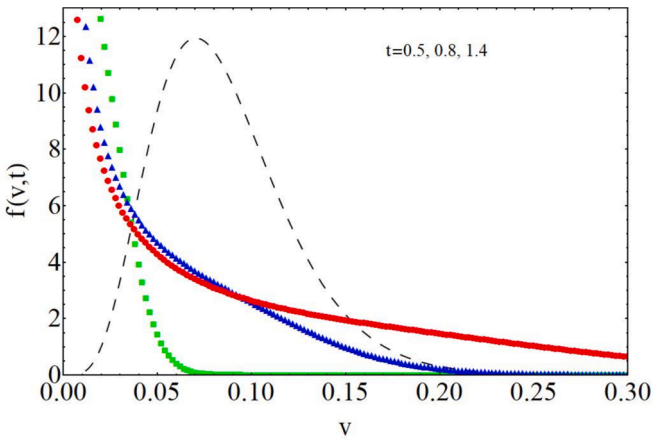

Fig. 8. PDFs for KJMA growth where the $f_\tau's$ are given by one-parameter gamma distribution. The parameter is τ-dependent according to the function of Fig. 7. Time values are: $t = 0.5$(blue solid triangles), $t = 0.8$ (green solid squares) and $t = 1.4$ (red solid circles). The asymptotic PDF for site saturated nucleation, namely the one parameter Gamma distribution with $\alpha_{3D} = 5.586$, is displayed as dashed line.

can be computed for a given f_τ and then compared to the data. In the case of slow varying nucleation rate, information on the $\tau-$ PDF could be gained by measuring the PDF in the low time domain where $I(t)$ and f_τ are nearly decoupled in the PDF expression.

We point out that the verification of the accord between experimental distributions and analytical PDFs (such as those discussed in this paper) is by no means trivial. In fact, the accord with the data can be eventually deemed using statistical approaches as discussed, for example, in [29,30]. In this context, it is worth quoting the recent work by Sun and Zangari [31] who presented a detailed modeling of the PDFs of electrodeposited particles, using lognormal, gamma and even Weibull distributions [32].

In ref. [33–35] the crystal size distribution functions of diamond crystals – grown by HFCVD (hot filament chemical vapor deposition) and MPCVD (microwave plasma CVD) on Si substrate – have been measured together with microscopic growth law and nucleation kinetics that was obtained by direct counting of crystals. The experimental crystal size distribution functions exhibit a power law behavior that has been interpreted, in ref. [36], based on Eq. (17).

The approach presented in sect.2.2 can be employed to have an insight into the growth kinetics when the PDF is known, and fluctuations are negligible. For instance, constant nucleation rate and a growth rate of crystal of the form $\frac{dv}{dt} \propto e^{\alpha v}$ (with constant α) leads to the exponential PDF, $f \propto e^{-\alpha v}$ (see [16] for the PDF expression for growth rate depending on crystal size). On the other hand, similar PDF is also consistent with an exponential decay of the nucleation rate, $I \propto e^{-\tau/\tau_N}$, and a logarithmic behavior of crystal growth with finite asymptotic size. Notably, this kind of distribution has been measured in experiments on crystal (plagioclase) formation during cooling of basaltic liquid, under isothermal and non-isothermal conditions [37,38]. Furthermore, for a constant rate of crystal growth and an exponential decay (in time) of the nucleation rate, the PDF increases exponentially up to the maximum crystal size. On the other hand, constant rates of both nucleation and growth imply a uniform PDF, if fluctuations are negligible.

In conclusion, in this paper we derive the FP equation for modeling the PDF of crystal size in phase transformations ruled by progressive nucleation and growth. The PDF is modeled as the superposition of the PDF of τ-crystals (τ-PDF). It is shown that the coefficients of growth and diffusion of the FP equation are appropriate averages of the f_τ. The functional form of the coefficients is investigated for the Gaussian, lognormal and gamma τ-PDFs. For time dependence of growth and fluctuation terms in accord with a simple exponential, the f_τ is either

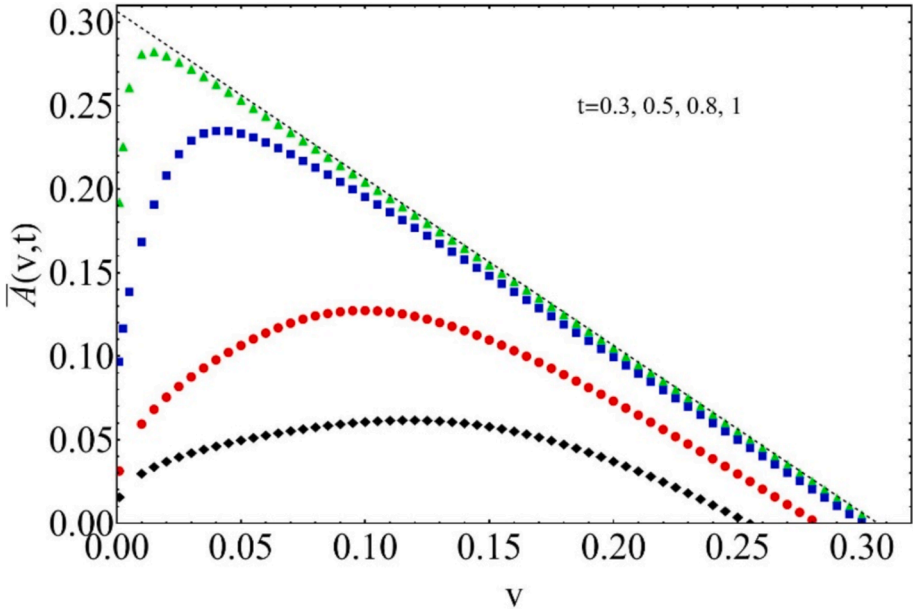

Fig. 9. Trend of the average value of A coefficient (for κ=1) with crystal volume, for several values of reduced time, t: $t = 0.3$(green triangles), $t = 0.5$ (blue solid squares), $t = 0.8$ (red solid circles), and $t = 1$ (black solid diamonds). The black dashed line is the function $A_0 = \overline{v}(\infty, 0) - v$, that is the limit of $\overline{A}$ for $t \to 0$.

Gaussian or lognormal, subject to the dependence of the coefficients with crystal size (sections 2.3.1 and 2.3.2.1), where the nucleation rate matches a stretched exponential. For size independent coefficients (section 2.2) and vanishing fluctuations, lognormal-like PDF stems from the functional form of the nucleation rate, that is a stretched exponential with $n = 2$ [12]. In fact, in the absence of fluctuations the PDF is a truncated lognormal where the cut-off in the volume domain is removed once fluctuations are included. This also occurs for the lognormal f_τ (section 2.3.2.1) where, in the absence of fluctuations, the volume cannot exceed the value $\overline{v}(0, \infty) = e^{\omega \tau_G}$. However, in this limiting case the whole distribution is not lognormal; its functional form is determined by the nucleation rate. We found that the time constant for nucleation and the strength of the fluctuation affect the distribution to a greater extent. On the other side, the time constant for fluctuation does not affect the distribution, markedly, apart from the lognormal case at low τ_F' (section 2.3.2.1).

For KJMA compliant transformations the τ-PDF is the one-parameter gamma distribution in which the parameter is a function of actual time and birth time of nuclei. At odd with the previous cases, the $A_\tau(v, t)$ coefficient, entering the FP equation for f_τ, depends on τ. It is found that in this case the coefficient for the FP equation of the whole PDF needs to be computed as τ-average of A_τ over the $[I(\tau) f_\tau]$ function. Computations of the mean growth rate, $\overline{A}$, as a function of time and crystal volume, have been done. As time increases the $\overline{A}$ *vs* v function deviates from the initial linear trend $\overline{A}(v, t \to 0) = A_0(v, \infty) = \overline{v}(\infty, 0) - v$, giving rise to maximum in the v domain and a decreasing $\overline{A}$ for given v.

CRediT authorship contribution statement

M. Tomellini: Writing – review & editing, Writing – original draft, Validation, Software, Methodology, Investigation, Formal analysis, Data curation, Conceptualization. **M. De Angelis:** Writing – review & editing, Writing – original draft, Visualization, Software, Methodology, Data curation.

Declaration of competing interest

The authors declare that they have no known competing financial interests or personal relationships that could have appeared to influence the work reported in this paper.

Acknowledgements

M.D.A. work has been carried out within the framework of the XXXIX Doctoral program in Chemical Sciences, Department of Chemical Science and Technologies, University of Rome Tor Vergata. The PhD grant has been partially funded by ENEA, Italian National Agency for New Technologies, Energy and Sustainable Economic Development.

The authors acknowledge Grant MUR Dipartimento di Eccellenza 2023-27 X-CHEM project "eXpanding CHEMistry: implementing excellence in research and teaching".

Appendices

A) Definition of averages over nucleation rate

Let us consider the probability entering Eq. (9):

$$\frac{I(\tau) f_\tau(v, t) d\tau}{\int I(\tau) f_\tau(v, t) d\tau} = \frac{I(\tau) f_\tau(v, t) d\tau dv}{dv \int I(\tau) f_\tau(v, t) d\tau}. \tag{A1}$$

The numerator in the second fraction is equal to the number of crystals nucleated between $\tau, \tau + d\tau$ with volume, at time t, in the range $v, v + dv$. In fact, $f_\tau(v, t) dv$ is the conditional probability a τ-nucleus, (i.e. formed between $\tau, \tau + d\tau$) has volume in the range $v, v + dv$ (at time t), i.e. $\frac{\Delta N(\tau, \tau + d\tau; v, v + dv)}{I(\tau) d\tau} = f_\tau(v, t) dv$, from which $\Delta N(\tau, \tau + \tau; v, v + dv) = I(\tau) f_\tau(v, t) d\tau dv$.

The denominator in the last fraction of Eq. (A1) is equal to the total number of crystals, at time t, with volume in the range $v, v+dv$: $dv\int_0^t I(\tau)f_\tau(v,t)d\tau = \Delta N(0,t;v,v+dv)$. As a consequence, the ratio above equals $\frac{\Delta N(\tau,\tau+d\tau;v,v+dv)}{\Delta N(0,t;v,v+dv)}$ that is the probability that a nucleation event occurs between τ and $\tau+d\tau$ and leads to a nucleus with volume in the range $(v, v+dv)$ at time t.

B) Solution of the FP equation for size-independent a and b coefficients

In this Appendix we discuss the solution of Kolmogorov's second equation for $f_\tau(v,t)$ in the limiting case of size independent a and b coefficients:

$$\frac{\partial f_\tau(v,t)}{\partial t} = -\frac{\partial[a_\tau(t)f_\tau(v,t)]}{\partial v} + \frac{\partial^2[b_\tau(t)f_\tau(v,t)]}{\partial v^2}, \tag{B1}$$

with $b_\tau(t) = B_\tau(t)/2$ and initial condition $f_\tau(v,\tau) = \delta(v-v_0)$. The Fourier transform of this equation, in the v variable, gives the following ordinary differential equation ($t > \tau$),

$$\frac{\partial f_\tau(\omega,t)}{\partial t} = -ia_\tau(t)\omega f_\tau(\omega,t) - \omega^2 b_\tau(t) f_\tau(\omega,t) \tag{B2}$$

with solution $f_\tau(\omega,t) = e^{-i\omega[v_0+\varphi_1(t,\tau)]}e^{-\omega^2\varphi_2(t,\tau)}$ where $\varphi_1(t,\tau) = \int_\tau^t a_\tau(x)dx$ and $\varphi_2(t,\tau) = \int_\tau^t b_\tau(x)dx$. The inverse Fourier transform of Eq. (B2) eventually provides,

$$f_\tau(v,t) = \frac{1}{\sqrt{4\pi\varphi_2}}e^{-\frac{(v_0+\varphi_1(t,\tau)-v)^2}{4\varphi_2}}. \tag{B3}$$

For $a_\tau(t) \equiv a(t) = \gamma e^{-\alpha t}$ the quantity $v_0+\varphi_1(t,\tau) = \xi(t,\tau) = v_0+\frac{\gamma}{\alpha}(e^{-\alpha\tau}-e^{-\alpha t})$ is the average value of v over f_τ. The Dirac delta distribution is recovered in the limit $\varphi_2 \to 0$ (i.e. $B \to 0$).

C) Solution of the FP equation for $a = a_1(t)v$ and $b = 0$

In this case the FP equation is

$$\frac{\partial f(v,t)}{\partial t} = -\frac{a_1(t)\partial[vf(v,t)]}{\partial v}. \tag{C1}$$

By setting $a_1(t)\partial t = \partial t'$ and $F(v,t') = vf(v,t(t'))$ the equation becomes,

$$\frac{\partial F(v,t')}{\partial t'} = -\frac{\partial[F(v,t')]}{\partial \ln v}. \tag{C2}$$

The solution of Eq. (C2) is in the form $F = \Phi(\ln v - t')$, namely $f(v,t) = \frac{1}{v}\Phi(\ln v - \ln u(t))$, with $\ln u(t) = \int_0^t a_1(x)dx$. Therefore, the PDF is conserved in time and for Dirac delta PDF, at $t = 0$, $\Phi(\bullet) = \delta(\bullet)$ and the solution is $f(v,t) = \frac{1}{v}\delta(\ln v - \ln\bar{v}(t))$, where $u(t)$ is the average value of v (Eq. (25a)).

Appendix A. Supplementary data

Supplementary data to this article can be found online at https://doi.org/10.1016/j.jcrysgro.2024.127970.

Data availability

Data will be made available on request.

References

[1] S. Torquato, H.W. Haslach Jr, Random heterogeneous materials: microstructure and macroscopic properties, Appl. Mech. Rev. 55 (2002) B62–B63.

[2] K.K. Alaneme, E.A. Okotete, Recrystallization mechanisms and microstructure development in emerging metallic materials: A review, J. Sci.: Adv. Mater. Devices 4 (2019) 19–33.

[3] B.R. Lawn, R.F. Cook, Probing material properties with sharp indenters: a retrospective, J. Mater. Sci. 47 (2012) 1–22, https://doi.org/10.1007/s10853-011-5865-1.

[4] M. Castro, A. Sánchez, F. Domínguez-Adame, Lattice model for kinetics and grain-size distribution in crystallization, Phys. Rev. B 61 (2000) 6579–6586, https://doi.org/10.1103/PhysRevB.61.6579.

[5] P.R. Rios, J.D.C.P.T.D. Oliveira, V.T.D. Oliveira, J.A.D. Castro, Microstructural descriptors and cellular automata simulation of the effects of non-random nuclei location on recrystallization in two dimensions, Materials Research 9 (2006) 165–170.

[6] D. Crespo, T. Pradell, Evaluation of time-dependent grain-size populations for nucleation and growth kinetics, Phys. Rev. B 54 (1996) 3101–3109, https://doi.org/10.1103/PhysRevB.54.3101.

[7] D. Crespo, T. Pradell, M.T. Clavaguera-Mora, N. Clavaguera, Microstructural evaluation of primary crystallization with diffusion-controlled grain growth, Phys. Rev. B 55 (1997) 3435–3444, https://doi.org/10.1103/PhysRevB.55.3435.

[8] J. Farjas, P. Roura, Cell size distribution in a random tessellation of space governed by the Kolmogorov-Johnson-Mehl-Avrami model: Grain size distribution in crystallization, Phys. Rev. B 78 (2008) 144101, https://doi.org/10.1103/PhysRevB.78.144101.

[9] E. Pineda, P. Bruna, D. Crespo, Cell size distribution in random tessellations of space, Phys. Rev. E 70 (2004) 066119, https://doi.org/10.1103/PhysRevE.70.066119.

[10] A.N. Shiryayev, Selected works of AN Kolmogorov: Volume II probability theory and mathematical statistics, Springer Science & Business Media, 1992. https://books.google.com/books?hl=it&lr=&id=04R8mqrUIb0C&oi=fnd&pg=PR1&dq=Selected+works+of+A.N.+Kolmogorov,+Vol.+II,+Probability+Theory+and+Mathematical+Statistics,+A.N.+Shiryayev+(Ed),+Kluwer+Academic+Publisher+1992,+Dordrecht,+Boston,+London,+chapter+9.&ots=kRgldDxpQb&sig=S07XP5lXCjhJ4XR1_wLvMajeyyo (accessed July 31, 2024).

[11] N.G. Van Kampen, Stochastic processes in physics and chemistry, Elsevier, 1992. https://books.google.com/books?hl=it&lr=&id=3e7XbMoJzmoC&oi=fnd&pg=PP2&dq=1)%09N.G.+Van+Kampen,+Stochastic+Processes+in+Physics+and+Chemistry,+North+Holland+Publishing+Company,+1981,+Amsterdam,+New+York,+Oxford&ots=Afu5vZpcpM&sig=aUyqnQd04VWf9DwGBFJE-IV7uRU (accessed July 31, 2024).

[12] R.B. Bergmann, A. Bill, On the origin of logarithmic-normal distributions: An analytical derivation, and its application to nucleation and growth processes, J. Crystal Growth 310 (2008) 3135–3138.

[13] A. Bill, R.B. Bergmann, Development of the Grain Size Distribution During the Crystallization of an Amorphous Solid, MRS Online Proceedings Library (OPL) 1308 (2011) mrsf10-1308.

[14] V.G. Dubrovskii, Analytic form of the size distribution in irreversible growth of nanoparticles, Phys. Rev. E 99 (2019) 012105, https://doi.org/10.1103/PhysRevE.99.012105.

[15] M. Tomellini, Fokker-Planck equation for the particle size distribution function in KJMA transformations, Physica A: Statistical Mechanics and Its Applications 615 (2023) 128515.

[16] M. Tomellini, On the grain size distribution function in KJMA compliant growth, Journal of Crystal Growth 584 (2022) 126579.
[17] D. Hömberg, F.S. Patacchini, K. Sakamoto, J. Zimmer, A revisited Johnson–Mehl–Avrami–Kolmogorov model and the evolution of grain-size distributions in steel, IMA Journal of Applied Mathematics 82 (2017) 763–780.
[18] E.V. Makoveeva, D.V. Alexandrov, A complete analytical solution of the Fokker-Planck and balance equations for nucleation and growth of crystals, Phil. Trans. R. Soc. A. 376 (2018) 20170327, https://doi.org/10.1098/rsta.2017.0327.
[19] E. Pineda, D. Crespo, Temporal evolution of the domain structure in a Poisson-Voronoi nucleation and growth transformation: Results for one and three dimensions, Phys. Rev. E 78 (2008) 021110, https://doi.org/10.1103/PhysRevE.78.021110.
[20] B. Rheingans, E.J. Mittemeijer, Phase Transformation Kinetics: Advanced Modeling Strategies, JOM 65 (2013) 1145–1154, https://doi.org/10.1007/s11837-013-0674-4.
[21] P. Bruna, D. Crespo, R. González-Cinca, E. Pineda, On the validity of Avrami formalism in primary crystallization, Journal of Applied Physics 100 (2006). https://pubs.aip.org/aip/jap/article/100/5/054907/974226 (accessed July 31, 2024).
[22] J.S. Blázquez, F.J. Romero, C.F. Conde, A. Conde, A Review of Different Models Derived from Classical Kolmogorov, Johnson and Mehl, and Avrami (KJMA) Theory to Recover Physical Meaning in Solid-State Transformations, Physica Status Solidi (b) 259 (2022) 2100524, https://doi.org/10.1002/pssb.202100524.
[23] M. Fanfoni, M. Tomellini, The Johnson-Mehl- Avrami-Kohnogorov model: A brief review, Nouv Cim D 20 (1998) 1171–1182, https://doi.org/10.1007/BF03185527.
[24] M. Tomellini, M. Fanfoni, Why phantom nuclei must be considered in the Johnson-Mehl-Avrami-Kolmogoroff kinetics, Phys. Rev. B 55 (1997) 14071–14073, https://doi.org/10.1103/PhysRevB.55.14071.
[25] N.V. Alekseechkin, Extension of the Kolmogorov–Johnson–Mehl–Avrami theory to growth laws of diffusion type, J. Non-Crystalline Solids 357 (2011) 3159–3167.
[26] M.P. Shepilov, On calculation of the transformation kinetics for models with the diffusional law of growth of new-phase precipitates, Crystallography Reports 50 (2005) 513–516.
[27] A. Korobov, Boundaries, kinetic properties, and final domain structure of plane discrete uniform Poisson-Voronoi tessellations with von Neumann neighborhoods, Phys. Rev. E 79 (2009) 031607, https://doi.org/10.1103/PhysRevE.79.031607.
[28] A. Pimpinelli, T.L. Einstein, Capture-zone scaling in island nucleation: universal fluctuation behavior, Phys. Rev. Lett. 99 (2007) 226102, https://doi.org/10.1103/PhysRevLett.99.226102.
[29] M.F. Vaz, M.A. Fortes, Grain size distribution: The lognormal and the gamma distribution functions, Scripta Metallurgica 22 (1988) 35–40.
[30] M.D. Higgins, Verification of ideal semi-logarithmic, lognormal or fractal crystal size distributions from 2D datasets, Journal of Volcanology and Geothermal Research 154 (2006) 8–16.
[31] Y. Sun, G. Zangari, Observation of Weibull, Lognormal, and Gamma Distributions in Electrodeposited Cu and Cu-Ag Particles, Materials 16 (2023) 6452.
[32] M. Fanfoni, B. Bonanni, R. Martini, S. Addessi, C. Goletti, A. Sgarlata, Weibull function to describe the cumulative size distribution of clumps formed by two-dimensional grains randomly arranged on a plane, Phys. Rev. E 109 (2024) 044131, https://doi.org/10.1103/PhysRevE.109.044131.
[33] M. Tomellini, R. Polini, V. Sessa, A model kinetics for nucleation at a solid surface with application to diamond deposition from the gas phase, Journal of Applied Physics 70 (1991) 7573–7578.
[34] J.C. Arnault, S. Saada, S. Delclos, L. Intiso, N. Tranchant, R. Polini, P. Bergonzo, In situ study of the initial stages of diamond deposition on 3C–SiC (100) surfaces: Towards the mechanisms of diamond nucleation, Diamond and Related Materials 16 (2007) 690–694.
[35] X. Jiang, K. Schiffmann, C.-P. Klages, Nucleation and initial growth phase of diamond thin films on (100) silicon, Phys. Rev. B 50 (1994) 8402–8410, https://doi.org/10.1103/PhysRevB.50.8402.
[36] M. Tomellini, M. Fanfoni, On the size distribution function of diamond nano-crystals grown on surfaces, Diamond and Related Materials 19 (2010) 1135–1138.
[37] E. Pupier, S. Duchene, M.J. Toplis, Experimental quantification of plagioclase crystal size distribution during cooling of a basaltic liquid, Contrib Mineral Petrol 155 (2008) 555–570, https://doi.org/10.1007/s00410-007-0258-9.
[38] K.V. Cashman, Crystal size distribution (CSD) analysis of volcanic samples: advances and challenges, Frontiers in Earth Science 8 (2020) 291.